

Cite this: *RSC Adv.*, 2017, 7, 43464

## Preparation of MgO nanocrystals and catalytic mechanism on phenol ozonation

Bing Wang,<sup>\*ab</sup> Xingao Yuan Xiong, <sup>a</sup> Hongyang Ren<sup>ab</sup> and ZhiYu Huang<sup>a</sup>

This research aims to clarify the role of magnesium oxide as a catalyst in the catalytic ozonation process. Nano-sized magnesium oxide was prepared by the sol-gel method and characterized by X-ray diffraction (XRD) and scanning electron microscopy (SEM). The catalytic performance of magnesium oxide was tested for the removal of phenol. The effect of initial pH, MgO nanocrystal amount, radical scavenger (*t*-butanol) and  $R_{ct}$  was investigated to understand the catalytic ozonation mechanism of magnesium oxide with ozone. Experimental results illustrated that nano-sized magnesium oxide presented significant performance for the ozonation and catalyzed the removal of phenol from aqueous solution by ozonation with a radical pathway involving hydroxyl radicals, which was due to the activity of surface basic groups from magnesium oxide where the conversion of ozone to hydroxyl radicals occurred. Fourier transform infrared spectroscopy (FT-IR) and isoelectric point (IEP) analysis was applied to analyze the surface properties of the prepared nano-magnesium oxide. Activation energy ( $E_a$ ) was calculated based on the Arrhenius principle equation. It reveals that phenol could enhance the density of surface hydroxyl groups and the introduction of magnesium oxide into the ozonation system does not alter the activation energy. Therefore, the prepared powder was found to be an efficient and promising catalyst for ozonation.

Received 9th July 2017  
Accepted 28th August 2017

DOI: 10.1039/c7ra07553g

rsc.li/rsc-advances

### 1. Introduction

Ozonation is one of the best known AOPs (advanced oxidant processes) which has gained significant attention in recent years. The main characteristic of this process is the production of reactive radicals at ambient temperature and pressure, especially hydroxyl radicals which are the predominant species for the degradation of inhibitory and toxic contaminants in wastewater.<sup>1</sup> Considering that the reaction between refractory organics and ozone is slow and selective, catalysts have been introduced to the ozonation system to accelerate both the degradation of organic pollutants and the mineralization of organics, followed by decreased reaction time, thereby reducing the treatment cost.<sup>2,3</sup> This advanced technology has been successfully applied for the removal of organic compounds over the last few years.

Catalytic ozonation processes could be divided into homogeneous catalytic ozonation and heterogeneous catalytic ozonation on the basis of which facilitate the decomposition of ozone and the formation of hydroxyl radicals, transition ions or solid catalysts.<sup>2</sup> Compared to single ozonation, heterogeneous catalytic ozonation could increase oxidation rate and decrease

utilization efficiency of ozone, and compared with homogeneous catalytic ozonation, heterogeneous catalytic ozonation is characteristic of reclamation, lack of secondary pollution has been considered as a promising AOP for wastewater treatment.<sup>4-6</sup>

The key issue for catalytic ozonation processes is to find an efficient catalyst.<sup>6</sup> Many metal oxides such as  $MnO_2$ ,  $TiO_2$ ,  $CeO_2$ ,  $Al_2O_3$ ,  $FeOOH$ ,  $ZnO$ , also supported metal oxides  $Fe_2O_3/Al_2O_3@SBA-15$ ,  $CeO_2/TiO_2$ ,  $Mn/\gamma-Al_2O_3$  have been used as catalysts in ozonation process and the catalytic activities were measured for remove target compounds, such as oxalic acid, nitrobenzene, *p*-chlorobenzoic, fulvic acid.<sup>7-15</sup>

Magnesium oxide is an important functional metallic oxide with the nature of nontoxic, economical, and environment-friendly has been considered as a feasible choice for catalytic ozonation process. Even magnesite show prominent activity for the removal of phenol from saline wastewater.<sup>16</sup> Several works have been published so far on magnesium oxide used as catalyst in ozonation process. It has been verified that magnesium oxide could efficiently catalyze ozone to degrade coumarin, dye, and formaldehyde in aqueous solution.<sup>17-19</sup> The removal efficiencies of both pollutants and COD were significantly enhanced by using of magnesium oxide in the ozonation process.<sup>6</sup>

In recent years, nano-magnesium oxide has been synthesized by sol-gel process, precipitation method or calcination and tested in linezolid antibiotic, benzene, dye, phenol.<sup>16,18,20,21</sup> As expected, nano-magnesium oxide has exhibited higher

<sup>a</sup>School of Chemistry and Chemical Engineering, Southwest Petroleum University, No. 8 Xindu Avenue, Xindu District, Chengdu 610500, P. R. China. E-mail: wangb@swpu.edu.cn; Fax: +86 02883037306; Tel: +86 02883037303

<sup>b</sup>Sichuan Provincial Key Laboratory of Environmental Pollution Prevention on Oil and Gas Fields and Environmental Safety, Chengdu 610500, P.R. China



efficiency in wastewater treatment, owing to its high surface area and exposed surface active sites.<sup>22</sup> Also the stability of nano-magnesium oxide has been measured and the result show easily recyclable with no significant change in activity.<sup>23</sup> The nano-sized magnesium oxide could be regarded as a very potential and deserving candidate for use in the catalytic ozonation context due to these properties presented above.<sup>16</sup>

The understanding of the mechanisms of catalytic ozonation in the presence of magnesium oxide is vital. The way oxidizing organic molecules by direct oxidation and/or by indirect radical oxidation has been studied by several groups to explore which is responsible for the degradation of organic compounds, however the results were contradictory with magnesium oxide.<sup>24</sup> Ozonation in the presence of magnesium oxide provide fast degradation of refractory organics has been inconclusive as to whether the catalyst act as adsorbent for organic compounds or play a direct part in the decomposition process, or whether reduce the activation energy. It should be noting here that no report could be found on the possible change on activation energy.

As stated above, three aspects are mainly focused on as follows: (I) preparation of nano-sized magnesium oxide by a modified soft non aqueous sol-gel process and further evaluation of its activity by catalytic ozonation phenol simulation wastewater compared with other high activity metal oxides as well as ozonation alone. (II) Investigation of catalytic mechanism by qualitatively and quantitative analysis about surface hydroxyl of prepared magnesium oxide and identify of hydroxyl radicals in bulk solution including surface property, effect of initial pH, catalyst amount, *tert*-butanol and calculation of  $R_{ct}$ , as well as the stability of catalyst. (III) Development of Arrhenius type to describe activation energy with or without magnesium oxide is still required.

## 2. Experimental

### 2.1 Material and catalyst

The magnesium oxide used in this work were prepared by a non-aqueous sol-gel process which referred to others and made some improvements.<sup>25</sup> In a typical procedure, 10 g (0.1783 mol) KOH was placed in 100 mL methylbenzene under vigorous stirring, after continuous stirring for 12 h, 15 g (0.07378 mol)  $MgCl_2 \cdot 6H_2O$  was added to the solution and stirring for 5 h with reflux condensation, then ultrasound for 20 min. Finally, the precipitate was collected by centrifugation and was washed with deionized water and anhydrous ethanol several times in order to remove the surface impurities until constant pH and dry at 105 °C overnight. The precursor were calcined in an muffle furnace at 500 °C for 3 h (with an constant rate of 2 °C min<sup>-1</sup>) and naturally cooled to room temperature to given the final product.

### 2.2 Experimental procedure

All ozonation experiments were performed in a plexiglass cylindrical reactor with 1.3 L capacity (inner diameter: 250 mm, high: 900 mm) and washed severd times with deionised water

before reaction to remove interfering elements. Ozone was generated from pure oxygen by a CF-G-3-20g generator and residual gas exhausted from the reactor was decomposed in a 2% KI before releasing to the environment.

The sole and catalytic ozonation were conducted in a continuous aeration mode (Fig. 1). Solution and catalysts were introduced into the reactor. Turning on and regulating the ozone generator until reached a steady state, then ozone were bubbled into the stimulated wastewater through microporous aerator with continuous magnetic stirring. In addition, Orge *et al.* confirmed the stirring rate do not affect the reaction rate, internal mass transfer resistances were considered negligible also in the condition that avoid any external mass transfer resistance.<sup>23</sup> After reaction, samples were taken from the reactor at a given time and 0.025 mol L<sup>-1</sup> Na<sub>2</sub>SO<sub>3</sub> solution was used to quench ozone in the liquid phase remaining in the sample. Then samples were analyzed immediately after filtration through a membrane filter attached to a syringe to remove suspended particles from the solution.

The research of surface properties carried out in erlenmeyer flask with 1 L pure water and 1 L phenol solution (100 mg L<sup>-1</sup>), respectively. Then ozone was introduced to the bottom of solution through microporous aerator under soft magnetic stirring. Samples were collected at 2 min intervals and catalysts were separated through filter paper. Finally, the separated magnesium oxide were dried at 30 °C several days. All the experiments at ambient temperature and pressure.

### 2.3 Characterization of catalysts and analytical procedures

The X-ray diffraction (XRD) pattern of the magnesium oxide was recorded on diffractometer (PANalytical B.V, Netherlandish) using CuK $\alpha$  radiation ( $\lambda = 0.15418$  nm, 40 kV). The diffraction patterns were obtained by increasing  $2\theta$  from 10° to 80°. The morphology of the prepared powder was observed by scanning electron microscope (SEM, Quanta 450). The BET specific surface area ( $S_{BET}$ ) was determined by nitrogen adsorption at 77 K (ST-MP-9).

The concentration of phenol was determined by visible spectrophotometer, absorbance was measured at 510 nm in a 1.0 cm cell after the filtration of samples. The surface hydroxyl density of magnesium oxide was determined by infrared spectrometer (Beifen-Ruili Analytical Instrument Company, Beijing). Zeta potential was performed with a Zata PSLs 190 Plus potential analyzer (Brookhaven, American). Total organic

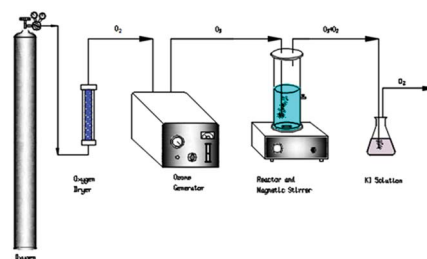


Fig. 1 Scheme of ozonation system.



carbon (TOC) of reaction mixture was detected with a TOC-VCPH analyzer (Shimadzu, Japan). The concentration of ozone in the solution was obtained through indigo method. The pH of the solution was measured by a PHS-3E pH meter (YokeChina instrument factory, Shanghai).

### 3. Results and discussion

#### 3.1 Characterization of catalysts

Fig. 2(a) shows the XRD spectra of the synthesized magnesium oxide samples. The main diffraction peaks observed at  $2\theta$  values of  $36.94^\circ$ ,  $43.01^\circ$ ,  $62.21^\circ$ ,  $74.62^\circ$ ,  $78.63^\circ$  can be indexed to the standard diffraction spectra of MgO powder (JCPDS card no. 45-0946) and were ascribed to the (111), (200), (220), (311), (222), respectively, indicating that the synthesized matter were pure magnesium oxide for there's no peaks resulting from impurities were observed. The Scherrer equation as shown in eqn (1):

$$D = \frac{K\lambda}{\beta \cos \theta} \quad (1)$$

where  $D$  is the median diameter of crystal particle,  $K$  is the a dimensionless constant and range from 0.89 to 1.39 (we used the value of 0.9);  $\lambda$  is the wavelength of X-ray diffraction light (0.15418 nm);  $\beta$  is the FWHM (full-width at half maximum) of the diffraction strongest peak;  $\theta$  is the location of the diffraction strongest peak.<sup>26</sup> According to Scherrer equation, the mean diameter average size of magnesium oxide was found to be 11.1 nm (using (200) plane).

The SEM image depicted in Fig. 2(b) and (c) was used to visualize the surface morphology of the prepared powder, and the image shows agglomerated and spherical nanocrystals, and

diameter is 50–100 nm. Therefore, the prepared powder is mainly composed of MgO nanospheres.

#### 3.2 Preliminary screening of catalysts

The catalytic activity of  $\text{Mn}_3\text{O}_4$ ,  $\text{Fe}_2\text{O}_3$ ,  $\text{ZnO}$ ,  $\text{MgO}$  were measured ( $C_{\text{phenol}} = 100 \text{ mg L}^{-1}$ ,  $C_{\text{catalyst}} = 40 \text{ mg L}^{-1}$ , ozone dosage:  $3.6 \text{ mg min}^{-1}$ ) compared with  $\text{O}_3$  alone in natural pH. Phenol was selected for this study because it is one of the most general compounds produced in the chemical, petrochemical, pharmaceutical industries.<sup>27</sup>

Fig. 3 shows the results obtained with ozone alone and in the presence of different catalysts indicating the catalysts do catalyse phenol removal, and magnesium oxide appears to catalyse the process most effectively. After 10 min reaction time, the degradation of phenol were in the sequence of:  $\text{O}_3/\text{MgO}$  (80.1%) >  $\text{O}_3/\text{ZnO}$  (68.3%) >  $\text{O}_3/\text{Fe}_2\text{O}_3$  (62.2%) >  $\text{O}_3/\text{Mn}_3\text{O}_4$  (59.8%) >  $\text{O}_3$  (57.3%). When reaction time was extend to 20 min, the removal rate of  $\text{O}_3/\text{ZnO}$  process reached 88.9% while  $\text{O}_3/\text{Mn}_3\text{O}_4$ ,  $\text{O}_3/\text{Fe}_2\text{O}_3$  processes were almost the same as single ozonation (81.8%), and  $\text{O}_3/\text{MgO}$  system achieved the best degradation 98.0% which was demonstrated that magnesium oxide could significantly enhance the oxidation efficiency of ozone. Among all the catalysts, magnesium oxide shows the best catalytic performance compared and selected as the catalyst of catalytic ozonation in the follow-up experiments.

Adsorption is an important factor influencing the removal rate of organic compounds in aqueous. It is widely accepted the mechanisms of heterogeneous catalytic ozonation that the chemisorption of organic molecules and/or ozone on the surface of the catalyst has to take place.<sup>28</sup> Chemisorption of ozone on the surface of catalyst leading to the formation of hydroxyl radicals followed radical mechanism and chemisorption of organic molecule as well as both organic molecule and ozone on the catalyst surface and subsequent organic matter, which were attacked by ozone molecules.<sup>29</sup> Also, some researchers have found that magnesium oxide were good adsorbent which could remove some pollutants from aqueous solutions. According to Fakhri,<sup>20</sup> magnesium oxide nanoparticles show the adsorption capacity for linezolid antibiotic removal, as well as  $\text{ZnO-MgO}$  nanocomposites. Hu *et al.* demonstrated that magnesium oxide has strong adsorption of hydrophobic alkaline organic compounds.<sup>30</sup> Wang Q. *et al.*

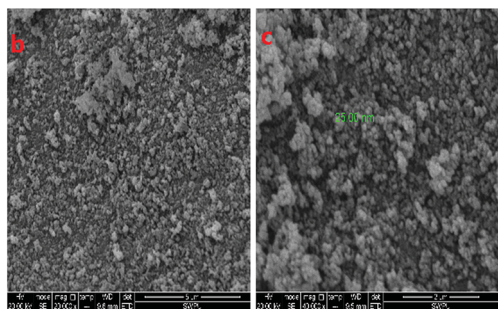
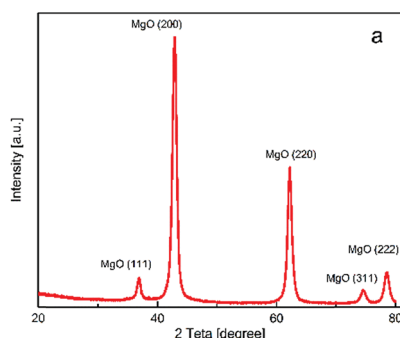


Fig. 2 (a) The XRD pattern; (b) and (c) SEM image of prepared MgO powder.

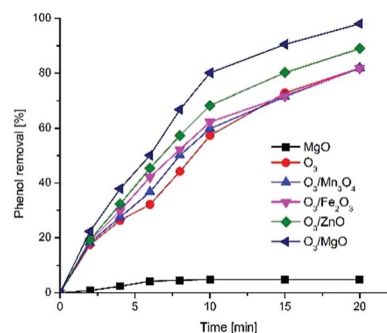


Fig. 3 Catalytic activity of  $\text{Mn}_3\text{O}_4$ ,  $\text{Fe}_2\text{O}_3$ ,  $\text{ZnO}$ ,  $\text{MgO}$ .



reported that the adsorption of dissolved organic carbon would reduce the specific surface area and active site,<sup>31</sup> leading to the decrease of removal efficiency in  $O_3/FeOOH$ ,  $O_3/MgO$  systems. In order to verify whether magnesium oxide act as adsorbent for phenol, further experiment without ozonation was performed in the same condition and the same reactor. As shown in Fig. 3, the absorption ability of magnesium oxide was very limited (less than 5%) may due to the competitive adsorption of water molecules which indicates that adsorption ability of magnesium oxide in this catalytic process to phenol was negligible. Therefore, the results might suggest that the degradation of phenol in solution may not be due to the absorption of magnesium oxide.

### 3.3 Catalytic activity of MgO

The ozonation with or without catalyst were conducted at pH of 6.8 under the same condition, and results are displayed in Fig. 4. Fig. 4(a) shows the removal percentage of phenol as a function of the catalytic activity, magnesium oxide has a pronounced effect on phenol degradation compared with ozone alone. For catalytic ozonation with magnesium oxides at 10 min, the degradation efficiency of phenol was 70.1%, which almost twice when compared with the sole ozonation (35.9%). In this case the assumption that hydroxyl radicals were produced and participated in the ozonation reaction when magnesium oxide was added should be in all probability. Staying with the result in last section that the effect of adsorption for phenol in the catalytic ozonation process could be neglected, thus the degradation of organic compounds might due to the oxidation by ozone and/or hydroxyl radicals. As shown in Fig. 4(b), the TOC removal in ozonation alone process are 2.7%, 3.8%, 5.6%, 7.7%, 9.3% at 2, 4, 6, 8, 10 min and in the presence of magnesium oxide increased by 2.2%, 3.6%, 6%, 5.9%, 13.2%, respectively, suggesting the prepared magnesium oxides clearly enhanced the mineralization efficiency of phenol. It is possible that the by-products of phenol degradation remains in solution, which was supported by the fact that the degree of mineralization was much lower than the phenol removal. The introduction of nano-magnesium oxide in ozonation process should provide fast degradation of phenol as well as mineralization compared with sole ozonation in the same condition, which demonstrates that nano-sized magnesium oxide was an active heterogeneous catalyst and play an important role in ozonation process.

### 3.4 Effect of catalysts amount

The catalytic activity depends on the surface area exposed in the solution and thus may predict that the oxidation of organic compounds strongly associated with the dosage of catalyst. Thus, the influence of dose of the prepared nanocrystal powder as well as analytical reagent (AR) was investigated.

Fig. 5 shows the percentage removal of phenol with time under different catalyst quantity (pH 6.9, ozone dosage:  $3.60 \text{ mg min}^{-1}$ ) and the reaction rate constants ( $k_{\text{obs}}$ ) of phenol removal rate have been determined in the following equation:

$$-\frac{d[\text{pH}]_t}{dt} = k_{\text{obs}}[\text{pH}]_0 \quad (2)$$

The data shown in Table 1 has evidenced that the prepared magnesium oxide have a better catalytic ability compared with MgO. Nanosized materials have unique physical and chemical properties, such as high  $S_{\text{BET}}$  and high reactivity.<sup>32,33</sup> The specific surface area of prepared powder is  $42.6 \text{ mg g}^{-1}$  while MgO (AR) is  $15.4 \text{ mg g}^{-1}$ , thus the results could be explained that prepared powder have higher surface area, signifying more surface basic groups which benefit catalytic ability. Moreover, this result was in agreement with the observation that the particle size decreasing, both catalytic activity and adsorption ability increased.<sup>34,35</sup> With respect to nano-sized magnesium oxide, the phenol removal rate rises with the increase of magnesium oxide dosage over 20 to  $40 \text{ mg L}^{-1}$  and then almost constant. Table 1 show clearly that the removal rate has increased from 90.59% to 97.7% and  $k_{\text{obs}}$  has increased from 0.1148 to 0.19105 in the presence of 20,  $40 \text{ mg L}^{-1}$  nano-magnesium oxide, respectively.

It has been verified that the degradation of phenol in ozonation system in the presence of nano-magnesium oxide did not

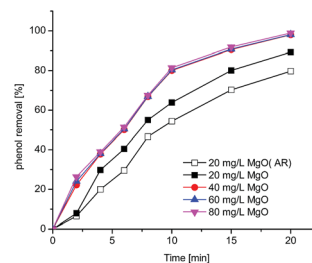


Fig. 5 The phenol removal rate by catalytic ozonation in the presence of 20, 40, 60,  $80 \text{ mg L}^{-1}$  prepared MgO and  $20 \text{ mg L}^{-1}$  AR MgO.

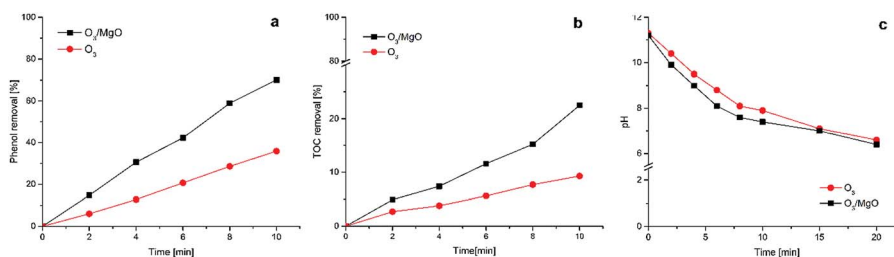


Fig. 4 The phenol (a) and TOC (b) removal rate in  $O_3$  and  $O_3/MgO$  systems; (c) the changes of pH over time.



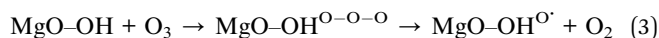


**Table 1** Pseudo-first-order rate constants of phenol degradation under different MgO dosage and  $S_{\text{BET}}$  of catalysts

	Concentration (mg L <sup>-1</sup> )	$R^2$	$k_{\text{obs}}$ (min <sup>-1</sup> )	BET surface area (m <sup>2</sup> g <sup>-1</sup> )
MgO (AR)	20	0.98743	0.09617	15.4
MgO	20	0.99448	0.1148	42.6
	40	0.967	0.19105	
	60	0.96588	0.19318	
	80	0.94457	0.21585	

involves the adsorption of phenol molecules onto catalyst. Thus, it could be hypothesized that ozone adsorbed on the surface of magnesium oxide would allow the generation of hydroxyl radicals which responsible for the oxidation of phenol. Generally ozone decomposition on the surface of a solid support, on Lewis centres, on non-dissociated hydroxyl groups of metal oxides, on basic centres of activated carbons.<sup>2,36–38</sup>

Isolated hydroxyls covered on magnesium oxide is responsible for ozone destruction. It is believed that  $k_{\text{obs}}$  depends on surface areas, with the increase of catalyst dosage, both the surface area exposed in bulk solution and the MgO-hydroxyl radicals which is the active centers that in favour of catalytic activity increased.<sup>6,9,18,39</sup> According to literature, the decomposition of ozone on the surface of catalysts leading to the formation of hydroxyl radical,<sup>2</sup> and the mechanism of the formation of radicals could be described as follows:



As shown in eqn (3) and (4), magnesium oxide act as an initiator in this process, ozone adsorbed on the surface of magnesium oxide and react with MgO-OH leading to the formation of MgO-OH<sup>O</sup> as the first step; then MgO-OH<sup>O</sup> attacked by ozone and hydroxyl radicals which is non-selective to organic compounds were generated.

In summary, it is possible to conclude that the increase of catalyst dosage made the surface hydroxyl group increased and integrated with ozone, which led to more non-selective radicals and high the removal rate. The reaction was dominant by catalyst dosage in this stage. Then continued addition of the catalyst, exposure of surface hydroxyl groups in the bulk solution increasingly but utilization of active centers almost constant with the fixed ozone concentration result in the removing rate at a same value.

### 3.5 Surface property of nano-magnesium oxide

Surface property of catalysts was the key factor of the catalytic activity.<sup>1</sup> Jun Chen *et al.* found a positive correlation between the catalytic activity of magnesium oxide and surface hydroxyl concentration.<sup>6</sup> In this section, experiments were conducted to quantitatively identify the hydroxyl radicals on the surface of magnesium oxide. Dried magnesium oxide used in catalytic ozonation in phenol and pure water systems were analyzed by

infrared spectrometer and the spectrum shown in Fig. 6. The appearance peaks located at 1637 and 3453 cm<sup>-1</sup> which are assigned to the face bending vibration and the stretching vibration respectively, both of which are the characteristic peaks of surface hydroxyl groups of H<sub>2</sub>O adsorbed on the surface of the catalyst.<sup>1,40,41</sup>

The peak observed at 1637 and 3453 cm<sup>-1</sup> in two systems (Fig. 6(a) and (b)) at 0 time evidenced that the presence of hydroxyl groups on the surface of magnesium oxide. The intensity of the peaks located at 1637 and 3453 cm<sup>-1</sup> (Fig. 6(a) and (b)) were increased with the increase of reaction time both in phenol and pure water systems, which indicates that the density of surface hydroxyl increased and consequent increase of absorbed (chemisorption) ozone content on the surface of magnesium oxide. Also the introduction of phenol improve the increasing range of peak value in heterogeneous catalytic ozonation system have been observed by comparing Fig. 6(a) and (b), which indicates that the catalyst in MgO-phenol system have higher surface hydroxyls density and adsorption capacity than the catalyst in MgO-pure water system. In terms of the mechanism about the formation of radicals presented in eqn (3) and (4), ozone adsorbed on surface hydroxyls and decomposed into radicals. It seems likely that part of the hydroxyl radicals produced by ozone decomposition released into solution degrading refractory organic matter and the rest existed on the surface of catalyst in forms of surface oxygenated radical species which enhance the density of surface hydroxyl groups.

It is difficult to explain the phenomenon that phenol can affect the amount of ozone on surface of magnesium oxide. Hence, an experiment was designed to study surface acid-basic properties of catalyst.

It is known that the surface property of catalyst could be affected by the pH of solution. Fig. 7 shows the effect of pH on zeta potential of magnesium oxide. This suggests that zeta potential rises over pH 6.3 to 12, and the isoelectric points (IEPs) for magnesium oxide were about 10.5. The pH of the reaction solution in this section was all under 10.5, where the surface would be positively charged in the form of MgO-OH<sub>2</sub><sup>+</sup>, while phenol has weak acidity which produced anions with hydrolysis reaction in solution. In phenol solution, more OH<sup>-</sup> are available and the attraction of OH<sup>-</sup> by surficial positive charges forms the convection of energy, which causes stronger collision between ozone and catalysts, hence more ozone were adsorbed on the surface basic group of magnesium oxide and decomposition into hydroxyl radicals according to eqn (3) and (4). This in turn indicates the ability of ozone decomposition on magnesium oxide would be strengthen in the process of ozonation.

In general, conclusion could be suggested as follows: (I) the decomposition of ozone on the surface of magnesium oxide occurs in pure water in heterogeneous catalytic ozonation process, demonstrating that magnesium oxide was able to decompose ozone into hydroxyl radicals, which was independent of phenol. (II) The presence of phenol in reaction system may promote the adsorption of ozone on the magnesium surface, and surface reaction would produce hydroxyl radicals which is less selective than ozone.



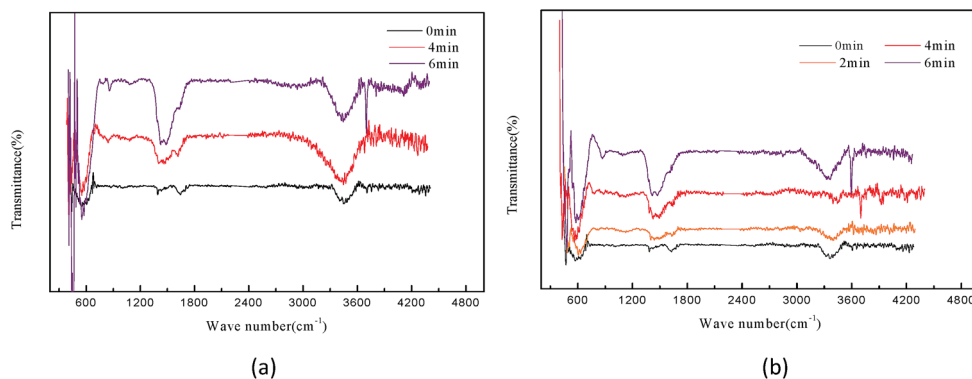


Fig. 6 FT-IR characterization: (a) MgO in MgO–phenol system at 0, 4, 6 min; (b) MgO in MgO–pure water system at 0, 2, 4, 6 min.

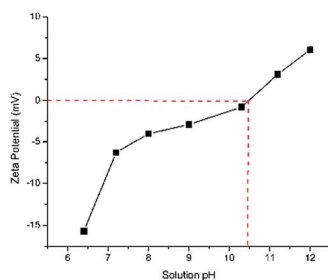


Fig. 7 Zeta potential of MgO at different pH.

### 3.6 Effect of initial pH

The initial pH of solution is a key factor for understanding the mechanisms of catalytic ozonation. As is already mentioned last section, pH of the reaction medium could affect the surface properties of catalyst and further determined the catalytic activity. The surface of magnesium oxide would be positively charged or negatively charged when  $pH_{pzc}$  above or below solution pH, respectively, while at  $pH_{pzc} = pH$  the surface of magnesium oxide is neutral. Furthermore, pH of bulk solution affects ozone decomposition. The presence of  $OH^-$  facilitating ozone decomposition into hydroxyl radicals, which could non-selectively oxidize organic compounds in bulk solution.<sup>42</sup> However, in acid environment, the degradation of organic matter mainly *via* a direct pathway such as electrophilic, nucleophilic and dipolar addition.<sup>43</sup>

Therefore, a series of experiments were conducted to evaluate the catalytic activity at different pHs. And the results presented in Fig. 8. As seen in Fig. 8, the phenol removal of both single ozonation and catalytic ozonation increased with the increasing initial solution pH from 1.7 to 11.23. And compared Fig. 8(a) and (b), the curve in the presence of magnesium oxide were higher than absence of magnesium oxide at the same condition, implying magnesium oxide could accelerate phenol degradation at wide range of pH and exhibited the most pronounced catalytic ability at pH 10.15, which is the nearest to  $pH_{pzc}$  (10.5). This phenomenon in accordance with the literature that neutral charged surface revealed a higher catalytic activity than both protonated and deprotonated surface for protonated surface is a weak nucleophile and deprotonated

surface cannot provide the electrophilic H to ozone.<sup>44</sup> However, the phenol removal with prepared magnesium oxide at pH 11.23 was slightly higher than pH 10.15. By considering the point that the phenol removal was caused by both the direct reaction with ozone and indirect reaction with hydroxyl radicals. Furthermore, hydroxyl radicals generated by two pathways: firstly, hydroxide ions in liquid initiated the chain reaction of ozone decomposition; the second was the surface acid–base property determined the catalytic activity, which has positive correlation with the ability to transform ozone molecule to hydroxyl radicals. This observation would be that the higher concentration of  $OH^-$  in bulk solution at pH 11.23 favorable for ozone decomposition and more hydroxyl radicals were generated in this condition, resulting in higher removal of organic matter.

The overall finding is that ozonation with prepared magnesium oxide could oxidize organic matter efficiently in both acid, neutral and alkaline environment, and the prepared powder showed the best catalytic activity when  $pH = pH_{pzc}$ .

### 3.7 Effect of TBA

The evidence presented above suggests that ozonation of phenol in the presence of magnesium oxide may dominated by hydroxyl radicals. To investigate whether hydroxyl radicals play a dominant role on ozonation process with magnesium oxide, TBA (*tert*-butanol), reaction rate constants of  $6 \times 10^8 M^{-1} s^{-1}$  with hydroxyl radicals and  $3 \times 10^{-3} M^{-1} s^{-1}$  with ozone, was selected as a radical probe due to the fact that the majority of

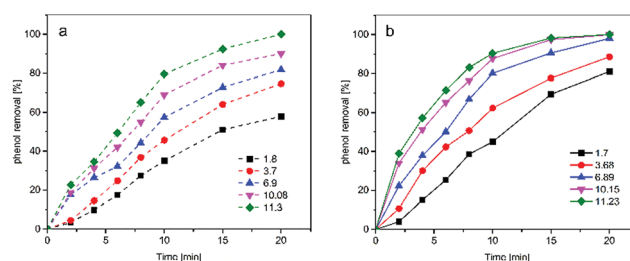


Fig. 8 Effect of initial pH on phenol removal in (a) single ozonation system; (b) catalytic ozonation system.



hydroxyl radicals could be hindered by TBA.<sup>45,46</sup> The effect of TBA on the catalytic ozonation and single ozonation was investigated and the results were presented in Fig. 9. It is observed that the phenol removal followed the sequences as:  $O_3/MgO > O_3/MgO + 12 \text{ mL TBA} > O_3 > O_3/MgO + 20 \text{ mL TBA} \approx O_3/MgO + 40 \text{ mL TBA}$ . The acceleration of phenol removal in the presence of magnesium oxide was in agreement with the observation shown in preliminary screening experiments and TBA indeed reduce the rate of phenol removal as expected which indicates the degradation of phenol in the  $O_3/MgO$  system might involve hydroxyl radicals. A similar observation reported by Kermani M *et al.* that both ozone molecules and radicals participated in the degradation of metronidazole by ozonation with magnesium oxide,<sup>47</sup> and the formation of hydroxyl radicals resulted from the decomposition of ozone which taking place on the catalyst surface.

Fig. 9 shows that the phenol removal rate were suppressed by the radical scavenger TBA in catalytic ozonation system, which further verified magnesium oxide catalyses a radical mechanism. It is clear that the removal rate of phenol in the presence of 12 mL TBA is less than  $O_3/MgO$  system. However, all above the curves of individual ozonation was apparently less than that with 20 mL TBA, revealing that the unreacted hydroxyl radicals existed in the solution with 12 mL TBA with a confirmation that the consumption of phenol in  $O_3/MgO$  system with 12 mL TBA may be due to the direct and indirect ozonation. Combining with the discussion above, the formation of hydroxyl radicals occurring through reaction between ozone and hydroxyl groups present on the surface of magnesium oxide, suggesting a fraction of ozone attacked phenol directly in bulk solution and the other fraction reacted with surface hydroxyl groups producing hydroxyl radicals which oxidated phenol soon. The concentration of phenol in the presence of 20, 40 mL TBA was reduced to the same extent, which might suggest the radicals in solution has been exhausted. This indicates the degradation of phenol with 20 and 40 mL TBA may be caused by the direct ozonation of ozone. The conclusion drawn from this experiments demonstrated that catalytic ozonation in the presence of magnesium oxide proceed with ozone molecule direct oxidation as well as hydroxyl radicals, and free radical mechanism may play a main role in this process.

### 3.8 Effect of pCBA

From the discussion above, it could be concluded that both ozone molecules and hydroxyl radicals contributes to the

degradation of phenol in the presence/absence of magnesium oxide and the heterogeneous catalytic ozonation process might be dominant by indirect way. *para*-Chlorobenzoic acid, which has a high reactivity with hydroxyl radicals and low reactivity with ozone molecule ( $k_{pCBA}/^{\bullet}OH = 5 \times 10^9 \text{ M}^{-1} \text{ s}^{-1}$ ,  $k_{pCBA}/O_3 = 0.15 \text{ M}^{-1} \text{ s}^{-1}$ ) was introduced into the ozonation systems either with or without magnesium oxide to quantitative analysis the amount of hydroxyl radicals in solution indirectly.<sup>48</sup>

The  $R_{ct}$ , which was proposed by Elovitz and von Gunten could be expressed as follows:<sup>49</sup>

$$R_{ct} = \frac{\int [^{\bullet}OH]dt}{\int [O_3]dt} \quad (5)$$

$$\ln\left(\frac{[pCBA]}{[pCBA]_0}\right) = -k_{OH/pCBA} R_{ct} \int [O_3]dt \quad (6)$$

Eqn (5) and (6) indicate the ratio of  $^{\bullet}OH$  radicals and ozone molecules exposed in solution and the transformation efficiency of ozone into  $^{\bullet}OH$  radicals, respectively.<sup>50</sup>

These experiments show that the decay of ozone molecules occurs mainly within two minutes and the decomposition rate decreased later could be owing to the reaction with pCBA and/or transformation of radicals. For the speculation that magnesium oxide was able to decompose ozone into hydroxyl radicals, the rate of ozone decomposition in two systems have also followed a same trend suggesting the hydroxyl radicals existed in solution without magnesium oxide.

The results presented in Fig. 10 shows that decrease of pCBA concentration in ozone alone system was not significantly while a noticeable decrease was registered with magnesium oxide in the experimental system. This phenomenon could be explained through two aspects compared with Fig. 10(a) as follows:

Firstly, the decomposition of ozone occurred independent of magnesium oxide which indicates radical reactions initiating, and the degradation of pCBA in ozone alone system follows hydroxyl radical pathway which proceeded in the bulk solution, and second, ozone adsorbed on the surface of magnesium oxide leading to the production of hydroxyl radicals which oxidize organic compound more efficient than ozone. Therefore, hydroxyl radicals abound in  $O_3/MgO$  system were responsible for the consumption of pCBA indicating the ozonation of pCBA

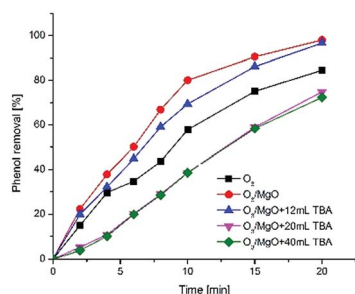


Fig. 9 Effect of TBA on phenol degradation.

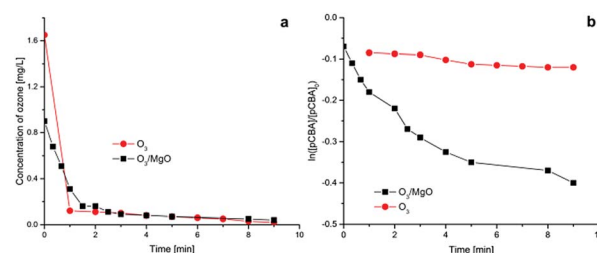


Fig. 10 The concentration of (a) aqueous ozone and (b) pCBA in ozonation alone and catalytic ozonation processes.



in this condition in the presence of magnesium oxide followed radicals mechanism.

The  $R_{ct}$  values were determined by eqn (6), as presented in Table 2. The  $R_{ct}$  value significantly increased with the adding of magnesium oxide which clearly revealed that both the transformation efficiency of ozone into hydroxyl radicals and the ratio of hydroxyl radicals and ozone molecules existed in bulk solution were approximately 3.8 times that without magnesium oxide. This result confirms that magnesium oxide could enhance the production of hydroxyl radicals, which was caused by the decomposition of ozone on the catalyst's surface and the degradation of organic compound in this system followed indirect reaction pathway with hydroxyl radicals.

### 3.9 Activation energy

The Arrhenius equation has been applied to chemical reaction and processes dependent of temperature. The  $E_a$  (activation energy ( $\text{J mol}^{-1}$ )) of ozonation in the presence/absence of magnesium oxide could be determined by Arrhenius equation:<sup>51–53</sup>

$$k = Ae^{\left(\frac{-E_a}{RT}\right)} \quad (7)$$

which could be transformed as:

$$\ln k = \ln A - \frac{E_a}{RT} \quad (8)$$

$R$  is the universal gas constant ( $8.314 \text{ J mol}^{-1} \text{ K}^{-1}$ ) and  $k(T)$  is the reaction rate at temperature  $T$  in  $^{\circ}\text{K}$ . Thus, a batch of experiments were conducted to provide  $k(T)$ .

Fig. 11 shows the expected results that high temperature could be contributed to the decomposition of ozone both in bulk solution and the surface of magnesium oxide, leading to the formation of hydroxyl radicals that should be responsible to the increase of degradation efficiency. Comparison of Fig. 11(a) and (b), clearly confirms that magnesium oxide do have a strong ability to catalyze ozone reaction for degradation of phenol which may take place on the surface of magnesium oxide. The reaction rate constant were calculated as presented in Table 3 according to the equation:

$$-\frac{d[\text{pH}]}{dt} = k(T)[\text{pH}]_0 \quad (9)$$

A plot of  $\ln k(T)$  versus  $1/T$  ( $T$  in  $^{\circ}\text{K}$ ) should be a straight line and the slope could be used to determine the activation energy of two processes in terms of temperature (Fig. 12) and the  $E_a$  of the

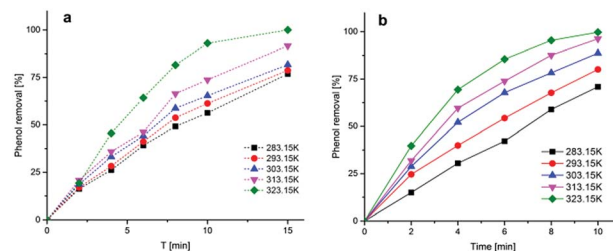


Fig. 11 Effect of temperature on phenol degradation by (a) ozonation alone; (b) catalytic ozonation.

Table 3 Pseudo-first-order rate constants of phenol degradation under different temperatures in ozonation alone system and catalytic ozonation system

$T (^{\circ}\text{K})$	$R^2$		$k(T) (\text{min}^{-1})$	
	$\text{O}_3$	$\text{O}_3/\text{MgO}$	$\text{O}_3$	$\text{O}_3/\text{MgO}$
283.15	0.9838	0.96722	0.09525	0.12195
293.15	0.9795	0.97637	0.10285	0.15556
303.15	0.99503	0.98836	0.1131	0.21451
313.15	0.96369	0.94235	0.16276	0.31282
323.15	0.92735	0.98161	0.25923	0.37145

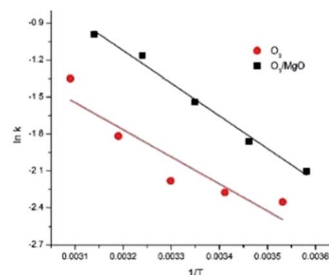


Fig. 12 Arrhenius plots of  $\ln k$  vs.  $(1/T)$ .

single ozonation and catalytic ozonation were calculated as  $18.279 \text{ kJ mol}^{-1}$ ,  $21.988 \text{ kJ mol}^{-1}$ , respectively. The subtraction of activation energy was  $3.709 \text{ kJ mol}^{-1}$ , indicating there's no significant difference in two systems which implies the presence of magnesium oxide could not reduce the activation energy of ozonation process. In contrast to our results, it has been reported by Ikhlaiq *et al.* that the ozonation of organic molecule in the presence of zeolite with the reduction of activation energy.<sup>17</sup>

Consequently, the high efficiency of this heterogeneous catalytic ozonation with magnesium oxide should be owing to the formation of hydroxyl radical resulted from the decomposition of ozone on the surface of magnesium oxide and further reaction between phenol and hydroxyl radicals might take place in the bulk solution.

### 3.10 Catalytic stability of the catalyst

Catalytic stability is a critical factor which directly related to the industrial application. It is therefore necessary to investigate

Table 2  $R_{ct}$  of ozonation alone system and catalytic ozonation system

	$R^2$	$k$		$R_{ct}$
		$(\text{mg L}^{-1})^{-1} \text{ min}^{-1}$	$\text{M}^{-1} \text{ s}^{-1}$	
$\text{O}_3$	0.94099	−0.0712	−59.2876	$1.14 \times 10^{-8}$
$\text{O}_3/\text{MgO}$	0.97396	−0.2697	−224.5768	$4.32 \times 10^{-8}$





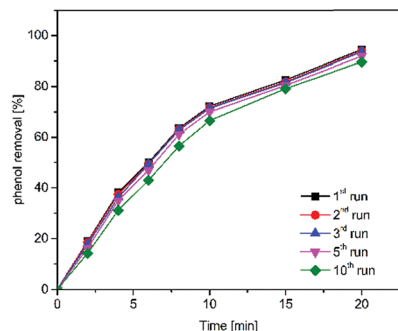


Fig. 13 Stability of prepared MgO for catalytic ozonation of phenol.

the catalytic activity in several repetitions of the synthesized powder.

As shown in Fig. 13, the removal of phenol followed the same trend in each run with the same batch of magnesium oxide in ozonation processes and reached 89.5% at 20 min in the tenthly recycling run while the phenol removal rate was 94.4% in the firstly use, which indicating that the catalytic activity of prepared magnesium oxide almost unchanged. These findings demonstrated that an excellent long-term catalytic ability for the prepared catalyst was along with the ozonation process in the degradation of organic compounds.

## 4. Conclusions

Based on experimental data, several conclusions can be drawn as follows: firstly, spherical nano-sized magnesium oxide catalyst was synthesized by a modified soft non aqueous sol-gel method with 50–100 nm in diameter and show the best performance compared with high activity metal oxide (e.g.  $\text{Mn}_3\text{O}_4$ ,  $\text{Fe}_2\text{O}_3$ ,  $\text{ZnO}$ ). Secondly, ozone degradation of phenol in the presence of nano-magnesium oxide dominated by a radical mechanism, and hydroxyl radicals was generated on the surface hydroxyl groups of magnesium oxide. Thirdly, magnesium oxide was able to transform ozone into hydroxyl radicals, and oxidizing phenol consequently. On the contrary, phenol can increase the density of surface hydroxyl. Fourthly, the enhancement of oxidation efficiency do not involves the change of activation energy, which could be evidenced by developing Arrhenius-type equation.

## Conflicts of interest

There are no conflicts to declare.

## Acknowledgements

This work was carried out with the financial support of the National Science and Technology Major Project of China (2016ZX05062).

## References

- 1 F. Qi, B. Xu, L. Zhao, Z. Chen, L. Zhang, D. Sun and J. Ma, *Appl. Catal., B*, 2012, **121**, 171–181.
- 2 J. Nawrocki and B. Kasprzyk-Hordern, *Appl. Catal., B*, 2010, **99**, 27–42.
- 3 C. Wu, C. Kuo and C. Chang, *J. Hazard. Mater.*, 2008, **154**, 748–755.
- 4 Q. Dai, J. Wang, J. Yu, J. Chen and J. Chen, *Appl. Catal., B*, 2014, **144**, 686–693.
- 5 Y. Zeng, Z. Liu and Z. Qin, *J. Hazard. Mater.*, 2009, **162**, 682–687.
- 6 J. Chen, S. Tian, J. Lu and Y. Xiong, *Appl. Catal., A*, 2015, **506**, 118–125.
- 7 H. Zhao, Y. Dong, P. Jiang, G. Wang, J. Zhang, K. Li and C. Feng, *New J. Chem.*, 2014, **38**, 1743–1750.
- 8 C. C. Wu, W. J. Huang and B. H. Ji, *J. Environ. Sci. Health, Part A: Toxic/Hazard. Subst. Environ. Eng.*, 2015, **50**, 1116–1126.
- 9 M. F. Pinheiro Da Silva, L. S. Soeira, K. R. P. Daghestanli, T. S. Martins, I. M. Cuccovia, R. S. Freire and P. C. Isolani, *J. Therm. Anal. Calorim.*, 2010, **102**, 907–913.
- 10 L. Mansouri, M. Sabelfeld, S. Geissen and L. Bousselmi, *Desalin. Water Treat.*, 2015, **53**, 1089–1100.
- 11 Y. Liu, S. Wang, W. Gong, Z. Chen, H. Liu, Y. Bu and Y. Zhang, *Catal. Commun.*, 2017, **89**, 81–85.
- 12 P. Gharbani and A. Mehrizad, *J. Saudi Chem. Soc.*, 2014, **18**, 601–605.
- 13 J. Bing, C. Hu, Y. Nie, M. Yang and J. Qu, *Environ. Sci. Technol.*, 2015, **49**, 1690–1697.
- 14 L. Chen, J. Li, M. Ge and R. Zhu, *Catal. Today*, 2010, **153**, 77–83.
- 15 Y. Wang, W. Yang, X. Yin and Y. Liu, *J. Environ. Chem. Eng.*, 2016, **4**, 3415–3425.
- 16 G. Moussavi, A. Khavanin and R. Alizadeh, *Appl. Catal., B*, 2010, **97**, 160–167.
- 17 A. Ikhlaiq, D. R. Brown and B. Kasprzyk-Hordern, *Appl. Catal., B*, 2012, **123**, 94–106.
- 18 G. Moussavi and M. Mahmoudi, *Chem. Eng. J.*, 2009, **152**, 1–7.
- 19 G. Moussavi, A. Yazdanbakhsh and M. Heidarizad, *J. Hazard. Mater.*, 2009, **171**, 907–913.
- 20 A. Fakhri and S. Behrouz, *Process Saf. Environ. Prot.*, 2015, **94**, 37–43.
- 21 S. Wang, Y. Wen, Z. Cui and Y. Xue, *J. Nanopart. Res.*, 2016, **18**, 1–9.
- 22 C. Xiong, W. Wang, F. Tan, F. Luo, J. Chen and X. Qiao, *J. Hazard. Mater.*, 2015, **299**, 664–674.
- 23 C. A. Orge, J. J. M. Orfao, M. F. R. Pereira, A. M. Duarte De Farias, R. C. Rabelo Neto and M. A. Fraga, *Appl. Catal., B*, 2011, **103**, 190–199.
- 24 K. He, Y. M. Dong, Z. Li, L. Yin, A. M. Zhang and Y. C. Zheng, *J. Hazard. Mater.*, 2008, **159**, 587–592.
- 25 A. Selvi and N. Das, *Environ. Prog. Sustainable Energy*, 2016, **35**, 706–714.
- 26 M. A. Alavi and A. Morsali, *Ultrason. Sonochem.*, 2010, **17**, 441–446.



- 27 Y. Dong, G. Wang, P. Jiang, A. Zhang, L. Yue and X. Zhang, *Bull. Korean Chem. Soc.*, 2010, **31**, 2830–2834.
- 28 F. P. Logemann and J. H. J. Annee, *Water Sci. Technol.*, 1997, **35**, 353–360.
- 29 B. Kasprzyk-Hordern, M. Ziólek and J. Nawrocki, *Appl. Catal., B*, 2003, **46**, 639–669.
- 30 J. Hu, Z. Song, L. Chen, H. Yang, J. Li and R. Richards, *J. Chem. Eng. Data*, 2010, **55**, 3742–3748.
- 31 Q. Wang, Z. Yang, B. Chai, S. Cheng, X. Lu and X. Bai, *RSC Adv.*, 2016, **6**, 14730–14740.
- 32 A. G. Gonçalves, J. J. Órfão and M. F. Pereira, *J. Environ. Chem. Eng.*, 2013, **1**, 260–269.
- 33 Y. Wang, Y. Xie, H. Sun, J. Xiao, H. Cao and S. Wang, *J. Hazard. Mater.*, 2016, **301**, 56–64.
- 34 W. J. Huang, G. C. Fang and C. C. Wang, *Colloids Surf., A*, 2005, **260**, 45–51.
- 35 S. Wang, Y. Wen, Z. Cui and Y. Xue, *J. Nanopart. Res.*, 2016, **18**, 15.
- 36 J. M. Roscoe and J. P. D. Abbatt, *J. Phys. Chem. A*, 2005, **109**, 9028–9034.
- 37 T. Zhang, C. Li, J. Ma, H. Tian and Z. Qiang, *Appl. Catal., B*, 2008, **82**, 131–137.
- 38 P. C. C. Faria, J. J. M. Orfao and M. F. R. Pereira, *Appl. Catal., B*, 2008, **79**, 237–243.
- 39 H. Petitjean, H. Guesmi, H. Lauron-Pernot, G. Costentin, D. Loffreda, P. Sautet and F. Delbecq, *ACS Catal.*, 2014, **4**, 4004–4014.
- 40 B. Liu, C. Li, Y. Zhang, Y. Liu, W. Hu, Q. Wang, L. Han and J. Zhang, *Appl. Catal., B*, 2012, **111**, 467–475.
- 41 J. M. Montero, M. A. Isaacs, A. F. Lee, J. M. Lynam and K. Wilson, *Surf. Sci.*, 2016, **646**, 170–178.
- 42 S. Afzal, X. Quan and J. Zhang, *Appl. Catal., B*, 2017, **206**, 692–703.
- 43 N. Graham, C. C. Jiang, X. Z. Li, J. Q. Jiang and J. Ma, *Chemosphere*, 2004, **56**, 949–956.
- 44 M. Pera-Titus, V. García-Molina, M. A. Baños, J. Giménez and S. Esplugas, *Appl. Catal., B*, 2004, **47**, 219–256.
- 45 G. V. Buxton, C. L. Greenstock, W. P. Helman and A. B. Ross, *J. Phys. Chem. Ref. Data*, 1988, **17**, 513–886.
- 46 W. R. Haag and J. Hoigné, *Water Res.*, 1983, **17**, 1397–1402.
- 47 M. Kermani, F. B. Asl, M. Farzadkia, A. Esrafil, S. S. Arian, M. Khazaei, Y. D. Shahamat and D. Zeynalzadeh, *Desalin. Water Treat.*, 2016, **57**, 16435–16444.
- 48 U. von Gunten, A. Driedger, H. Gallard and E. Salhi, *Water Res.*, 2001, **35**, 2095–2099.
- 49 M. S. Elovitz and U. von Gunten, *Ozone: Sci. Eng.*, 1999, **21**, 239–260.
- 50 H. Jung and H. Choi, *Appl. Catal., B*, 2006, **66**, 288–294.
- 51 L. Zhao, Z. Sun, J. Ma and H. Liu, *Environ. Sci. Technol.*, 2009, **43**, 2047–2053.
- 52 S. B. Mortazavi, G. Asgari, S. J. Hashemian and G. Moussavi, *React. Kinet., Mech. Catal.*, 2010, **100**, 471–485.
- 53 M. Peleg, M. D. Normand and M. G. Corradini, *Crit. Rev. Food Sci. Nutr.*, 2012, **52**, 830–851.

